buildings

MDPI

Article

Research on Parametric Vibration of a Steel Truss Corridor under Pedestrians Excitation Considering the Time-Delay Effect

Zhou Chen [1], Jiahao Wen [1], Deyuan Deng [2,3,*], Wei Dai [2], Siyuan Chen [4], Hanwen Lu [1] and Lingfei Liu [1]

[1] School of Transportation and Civil Engineering & Architecture, Foshan University, Foshan 528225, China
[2] School of Civil Engineering, Southeast University, Nanjing 211189, China
[3] China Construction Steel Structure Guangdong Corp, Huizhou 516200, China
[4] Guangdong Nanhai Construction Investment Development Co., Ltd., Foshan 528200, China
* Correspondence: deyuangdeng@fosu.edu.cn

Abstract: With the development of the Steel Truss Corridor (STC) toward long-span and gentle development, human-induced vibration often causes large lateral vibration problems and time-delay effects of the STC, which will have a non-negligible impact on the dynamic performance of the STC. In this paper, the parametric vibration model proposed by Piccardo is improved, and the nonlinear dynamic equation of the STC is established considering the longitudinal–lateral walking force coupled parametric vibration with the time-delay effect. Taking the Millennium STC as an example, the mechanism of lateral vibration under the time-delay effect is discussed by the numerical calculation method, and the influence of the time-delay effect on its dynamic response is analyzed. The results show that: considering the time-delay effect, when the frequency ratio $\theta/2\Omega = 1$, the value of the time-delay coefficient has no effect on the critical number of STCs in the parametric resonance region. As $\theta/2\Omega$ moves away from 1, the more significant the effect. When the STC begins to excite the parametric resonance phenomenon, the existence of the time-delay effect will change the time for the STC to reach a stable amplitude and suppress the lateral vibration of the STC. When the STC generates parametric vibration, the value of the time-delay coefficient has no effect on the nonlinear dynamic response of the STC. For STCs in both the nonparametric resonance region and the critical region, there is a pair of staggered critical bifurcation time-delay coefficients, which increase or decrease the vibration response.

Keywords: STC; time-delay; the critical number of people; bifurcation; dynamic stability

check for updates

Citation: Chen, Z.; Wen, J.; Deng, D.; Dai, W.; Chen, S.; Lu, H.; Liu, L. Research on Parametric Vibration of a Steel Truss Corridor under Pedestrians Excitation Considering the Time-Delay Effect. *Buildings* **2023**, *13*, 98. https://doi.org/10.3390/buildings13010098

Academic Editor: Krishanu Roy

Received: 7 November 2022
Revised: 24 December 2022
Accepted: 29 December 2022
Published: 30 December 2022

1. Introduction

The development of STCs with large spans, light flexibility [1], and low damping will inevitably reduce the structure's fundamental frequency. Structures with low frequencies are often prone to a series of vibration problems [2]. The lateral dynamic stability of STCs is a long-neglected problem [3], and how to explain and predict the sudden increase in lateral amplitude is a hot topic in the research on the dynamic stability of STCs [4]. Studies have shown that the longitudinal and lateral first-order frequencies of normal pedestrians walking are between 0.7 and 1.2 Hz [5]. When the fundamental STC frequency is in this range, the forced resonance theory with a frequency ratio of 1:1 can explain the mechanism of lateral dynamic instability occurring in low-frequency STCs. However, suppose the frequency ratio satisfies the 1:2 relationship. In that case, it is difficult for the forced vibration theory to provide a reasonable explanation and prediction of the mechanism of sizeable lateral instability occurring in STCs [6]. The study by Piccardo [7] illustrates that parametric vibrations can cause lateral dynamic instability in STCs, but it only considers the limitations of the effect of lateral pedestrians walking forces, which occur in three directions during the walking process [8]. The time-delay effect is a natural phenomenon present in the field of STCs [9]. Due to the complexity of the internal systems of STCs, the body's feedback regulation, and the lag in signal transmission when people are in contact with the STC, the time-delay effect is inevitable. If the inherent time-delay effect of STCs is not considered, it will inevitably significantly impact the dynamic performance and stability of STCs [10]. The time-delay effect of STCs depends on two factors: the difference in reaction time between pedestrians, which is not adjustable, and the external nature of the STC. Studies have shown that the properties and thickness of the STC deck material change the size of the time-delay coefficient; the thicker and softer the deck material, the greater the time-delay effect, which is a modifiable factor [11].

In this paper, the parametric vibration model proposed by Piccardo [12] is improved to establish a nonlinear dynamic equation for an STC considering the coupled longitudinal–lateral walking forces as parametric vibrations [13]. Firstly, the nonlinear dynamic equations for a simply supported STC are established based on the energy method by considering the vertical walking force as a uniform mass, the lateral walking force, and the longitudinal walking force as simple harmonic forces. The time-delay affects the dynamic instability region, the nonlinear dynamic response, and the stability of the Millennium STC.

2. Nonlinear Parametric Vibration Model for the STC

2.1. Basic Assumptions

The nonlinear dynamic equations for STCs under the action of pedestrians forces have prominent characteristics of pedestrians–Steel Truss Corridor dynamic interactions [14], and it is challenging to establish such equations directly [15]. Simply supported girder STCs are one of the more common forms of urban STC systems, so studying the dynamic stability of simply supported STCs is of more general application [16]. The pedestrians–Steel Truss Corridor dynamic interaction is first excluded to facilitate the study, and the following assumptions are made.

(1) The number of pedestrians is considered to be evenly distributed along the span of the STC.
(2) We ignore the effect of the pedestrians' forward direction on the three-way walking force.
(3) The STC modeling obeys the Euler–Bernoulli beams' assumption.
(4) We ignore the effect of the pedestrians' damping.

Based on the above assumptions, the longitudinal walking force of the pedestrians is equated to the simple harmonic force $Q_h(t)$, the lateral walking force of the pedestrians is equated to the uniform, simple harmonic force $Q_l(t)$, and the vertical walking force of the pedestrians is replaced by the uniform mass m. The longitudinal, lateral, and vertical displacements generated by the STC are expressed as u, w, and v. The force model of the STC is shown in Figure 1.

2.2. Dynamic Equilibrium Equations for STCs

Assuming that the section perpendicular to the beam axis before deformation and the section perpendicular to the beam axis after deformation remain unchanged, i.e., without considering the effect of shear deformation, the normal longitudinal strain at any point at this point is shown in Equation (1) [17].

$$\varepsilon(x,t) = \frac{\partial u}{\partial x} + \frac{1}{2}\left(\frac{\partial w}{\partial x}\right)^2 + z\frac{\partial^2 w}{\partial x^2}\cos\theta \approx \frac{\partial u}{\partial x} + \frac{1}{2}\left(\frac{\partial w}{\partial x}\right)^2 + z\frac{\partial^2 w}{\partial x^2}\left(1 - \frac{1}{2}\left(\frac{\partial w}{\partial x}\right)^2\right) \tag{1}$$

In Equation (1), t denotes time, $u(x,t)$ and $w(x,t)$ denote the displacements caused by the longitudinal and lateral walking forces, and θ is the angle of rotation of the cross-section around the oz direction.

At this point, the normal stress of the STC in the linear elastic range can be expressed as

$$\sigma(x,t) = E\varepsilon(x,t) \tag{2}$$

In Equation (2), E denotes the elastic modulus of the STC. Based on the principle of the energy method, the Lagrange equation for an STC under the action of walking forces is obtained in Equation (3).

$$L_a = T - U + V + D \tag{3}$$

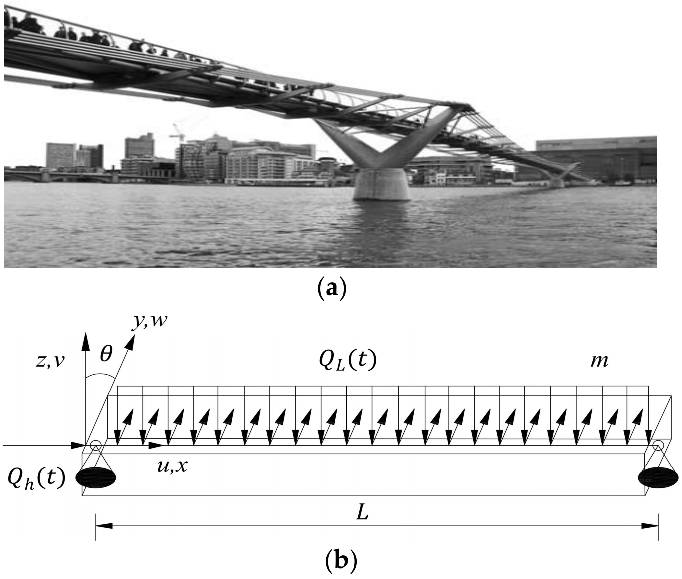

Figure 1. Physical drawing and mechanical model of simply supported STC considering longitudinal–lateral–vertical walking force. (**a**) Physical drawing. (**b**) Mechanical model.

In Equation (3), T, U, V, and D denote the kinetic energy, strain energy, work of conservative forces, and work of non-conservative forces (damping) of the vibrating system, respectively. Equation (4) represents the specific expressions for T, U, V, and D [17].

$$\begin{gathered} T = \frac{1}{2}(\rho_s A + m_p)\int_0^L \left((\frac{\partial u}{\partial t})^2 + (\frac{\partial w}{\partial t})^2 \right) dx \\ U = \frac{1}{2}\int_0^L \left\{ EA\left[\frac{\partial u}{\partial x} + \frac{1}{2}\left(\frac{\partial w}{\partial x}\right)^2 \right]^2 + EI\left(\frac{\partial^2 w}{\partial x^2}\right)^2 \left(1 - \frac{1}{2}\left(\frac{\partial w}{\partial x}\right)^2\right)^2 \right\} dx \\ V = \int_0^L [Q_h(t)u + Q_l(t)w] dx \\ D = -\mu \int_0^L \left[\frac{\partial u}{\partial t}u + \frac{\partial w}{\partial t}w \right] dx \end{gathered} \tag{4}$$

In Equation (4), ρ_s is the density per unit length of the STC material, A is the cross-sectional region of the STC, I is the cross-sectional moment of inertia, m_p is the mass of pedestrians per linear meter, and μ is the damping coefficient of the longitudinal and lateral of the STC.

From Hamilton's principle, the dynamical equilibrium equation of the system can be expressed as:

$$\int_{t_1}^{t_2} \delta L dt = \int_{t_1}^{t_2} \delta(T - U + V + D) dt = 0 \tag{5}$$

In Equation (5), δ is the Dirac function, and [t_1, t_2] denotes any time interval. Neglecting the effect of the lateral motion of the beam on the longitudinal motion and the longitudinal inertia of the beam, the geometrically nonlinear dynamic equations of the STC considering the longitudinal–lateral walking forces are obtained as: [17]

$$(\rho_s A + m_p)\frac{\partial^2 w}{\partial t^2} + \mu\frac{\partial w}{\partial t} + EI \cdot \left[\frac{\partial^4 w}{\partial x^4}\left(1 - (\frac{\partial w}{\partial x})^2\right) - \frac{\partial^2 w}{\partial x^2}\left(4\frac{\partial^3 w}{\partial x^3}\frac{\partial w}{\partial x} + (\frac{\partial^2 w}{\partial x^2})^2\right) \right] + Q_h L \frac{\partial^2 w}{\partial x^2} - \frac{3EA}{2}\frac{\partial^2 w}{\partial x^2}(\frac{\partial w}{\partial x})^2 = Q_l \tag{6}$$

Dillard [18] carried out experiments on the relationship between lateral forces and the lateral vibration velocity of a structure on a mobile platform in the laboratory. The experimental results show that the lateral walking forces of pedestrians are related to the lateral vibration velocity of the STC, i.e.,

$$Q_l(t) = \lambda\left(\alpha_{l1} + \alpha_{lv}\dot{w}\right)m_p g\cos(\omega_p t) \tag{7}$$

In Equation (7), $\alpha_{l1} = 0.04$ represents the dynamic load coefficient for pedestrians on fixed platforms and $\alpha_{lv} = 0.7$ is the dynamic load coefficient associated with the lateral vibration velocity of the structure. ω_p is longitudinal and lateral walking frequency. For girder STCs, where higher-order modes are less likely to occur and the higher-order frequencies are not within the range of pedestrians step frequencies, only the first-order mode is considered; thus,

$$w(x,t) = Y(t)\sin\left(\frac{\pi x}{L}\right) \tag{8}$$

In Equation (8), $Y(t)$ is the generalized coordinate of the first mode shape. Substituting Equation (8) into Equation (7) for modal coordinate transformation and integrating over the STC span L, the second-order variable coefficient ordinary differential equation for the longitudinal–lateral coupled parametric vibration of the STC is obtained as shown in Equation (9) [17].

$$\begin{array}{l}\ddot{Y}(t) + \left[\zeta_1 - \zeta_2\cos(\omega_p t)\right]\dot{Y}(t) + \omega_0^2\left[1 - 2\beta_1\cos(\omega_p t)\right]Y(t) + \beta_2 Y^3(t) - F_0\cos(\omega_p t) = 0 \\ \beta_1 = \frac{\lambda\alpha_{h1}m_p g L^3}{2\pi^2 EI},\ \beta_2 = \frac{\pi^4\left(EAL^2 - 2EI\pi^2\right)}{2L^6\left(\rho_s A + m_p\right)},\ \omega_0 = \sqrt{\frac{EI\pi^4}{L^4\left(\rho_s A + m_p\right)}} \\ \zeta_1 = 2\zeta_0\omega_0,\ \zeta_2 = \frac{\lambda\alpha_{lv}m_p g}{\rho_s A + m_p},\ F_0 = \frac{\pi\lambda\alpha_{l1}m_p g}{2\left(\rho_s A + m_p\right)}\end{array} \tag{9}$$

In Equation (9), ω_0 is the natural circle frequency of the first order of the STC considering the influence of pedestrians mass, ζ_0 is the damping ratio of the STC, $\zeta_2\cos(\omega_p t)\dot{Y}(t)$ is the parametric vibration of the STC by the pedestrians due to the lateral vibration velocity of the STC, $2w_0^2\beta_1\cos(\omega_p t)Y(t)$ is the parametric vibration due to the longitudinal pedestrians walking force, $\beta_2 Y^3(t)$ is the nonlinear elastic term in the equation, $F_0\cos(\omega_p t)$ is the forced vibration of the pedestrians walking, λ is the synchronous ratio of the pedestrians, α_{h1} is the longitudinal walking force dynamic load coefficient, α_{l1} is the lateral walking force dynamic load coefficient, ω_p is the longitudinal and lateral pedestrians step frequency, g is the gravitational acceleration, and α_{lv} is the dynamic load coefficient associated with the vibration velocity of the STC.

From Equation (9), it can be seen that there are nonlinear damping forces and nonlinear elastic forces in the equation. The nonlinear damping force indicates that the walking force in the synchronous state of the pedestrians will give the STC a negative damping, and when the negative damping cancels out the inherent positive damping of the STC, the STC enters an unstable state.

3. Parametric Vibration Equations for STC Taking into Account Time-Delay Effects

The correlation terms for pedestrians walking force excitation contain coefficients related to the time-delay effect τ ($\tau > 0$). Therefore, the equation is rewritten based on Equation (9) as a nonlinear parametric vibration equation for the STC, considering the time-delay effect.

$$\ddot{Y}(t) + \zeta_1\dot{Y}(t) + \omega_0^2 Y(t) + \beta_2 Y^3(t) = \cos\left[\omega_p(t-\tau)\right]\cdot\left[\zeta_2\dot{Y}(t-\tau) + 2\omega_0^2\beta_1 Y(t-\tau) + F_0\right] \tag{10}$$

3.1. Solution of Dynamically Unstable Regions Considering Time-Delay Effects

Based on the conclusions of Bolotin [19], omitting the effect of the nonlinear and forcing terms, Equation (10) can then be written as:

$$\ddot{Y}(t) + \zeta_1\dot{Y}(t) + \omega_0^2 Y(t) = \cos\left[\omega_p(t-\tau)\right]\left[\zeta_2\dot{Y}(t-\tau) + 2\omega_0^2\beta_1 Y(t-\tau)\right] \tag{11}$$

The Bolotin method is used to solve the second-order dynamical instability region of Equation (11), corresponding to a period of 2T. Let $Y(t)$ have a periodic solution with a period of 2T, whose expression for the Fourier series is:

$$Y(t) = \sum_{n}^{\infty}\left[a_n \sin\left(\frac{n\omega_p t}{2}\right) + b_n \cos\left(\frac{n\omega_p t}{2}\right)\right], n = 1,3,5,\cdots \tag{12}$$

In Equation (12), a_n and b_n are the coefficients of the periodic solution corresponding to the period 2π.

Taking n = 1 and n = 3, substituting into Equation (12), and taking the first and second derivatives for time t, we obtain the derived equation.

Substituting the periodic solution assumed by the derived equation into Equation (12), the system of system of homogeneous linear equations is obtained by trigonometric transformation, and the system of equations is written in a matrix-vector form. There exists a non-zero solution to the system of homogeneous linear equations only if the coefficient determinant is equal to zero.

$$\begin{gathered} \mathbf{A}\mathbf{x} = \mathbf{0} \\ \mathbf{x} = [a_3, a_1, b_1, b_3]^T \\ \mathbf{A} = \begin{bmatrix} \mathbf{A}_{11} & \mathbf{A}_{12} \\ \mathbf{A}_{21} & \mathbf{B}_{22} \end{bmatrix} \end{gathered} \tag{13}$$

Solving det(A) = 0 can obtain the second-order critical frequency equation corresponding to the periodic solution with a period of 2T.

3.2. Nonlinear Dynamic Response Solution Considering the Time-Delay Effect

For Equation (10), let $Y(t) = y_1, \dot{Y}(t) = y_2$ and expand $\cos[w_p(t-\tau)]$ by the Taylor series to obtain Equation (16).

$$\begin{aligned} &\dot{y}_2 = F_0\left(1 - \tfrac{w_p{}^2(t-\tau)}{2} + \mathrm{O}\left(\tfrac{w_p{}^4(t-\tau)^4}{24}\right)\right) - \zeta_1 y_2 \\ &+\zeta_2 y_2(t-\tau)\left(1 - \tfrac{w_p{}^2(t-\tau)}{2} + \mathrm{O}\left(\tfrac{w_p{}^4(t-\tau)^4}{24}\right)\right) - \omega_0^2 y_1 \\ &+2\omega_0^2\beta_1 y_1(t-\tau)\left(1 - \tfrac{w_p{}^2(t-\tau)}{2} + \mathrm{O}\left(\tfrac{w_p{}^4(t-\tau)^4}{24}\right)\right) + \beta_2 y_1{}^3 \end{aligned} \tag{14}$$

Ignoring dimensionless quantities, since Equation (14) has a unique equilibrium solution at the origin, Equation (14) is linearized at the origin to obtain its characteristic equation, order $1 - \frac{w_p{}^2(t-\tau)}{2} = k$, which gives

$$\lambda^2 + \left(\zeta_1 - \zeta_2 k e^{-\lambda\tau}\right)\lambda + \omega_0^2 = 0 \tag{15}$$

Let $\tau = 0$; thus, Equation (15) degenerates into ordinary differential equations

$$\lambda^2 + (\zeta_1 - \zeta_2 k)\lambda + \omega_0^2 = 0 \tag{16}$$

When $\zeta_1 - \zeta_2 k = 0$, Equation (16) has a pair of pure imaginary roots, i.e., $\lambda_{1,2} = \pm i w_0$. When $\zeta_1 - \zeta_2 k < 0$, it means that the real part of Equation (16) is greater than 0, the negative damping caused by the pedestrians' speed will aggravate the lateral dynamic instability of the STC; when $\zeta_1 - \zeta_2 k > 0$, it means that the real part of Equation (16) is less than 0, and the positive damping of the STC will slow down the lateral vibration of the STC. By Hopf's bifurcation theorem [20], bifurcation will occur near $\zeta_1 - \zeta_2 k = 0$.

Let $\lambda = iw(w > 0)$; then, substitute into Equation (16) and separate the real and imaginary parts of the equation such that k = 1, giving:

$$\begin{aligned} &-w^2 + \omega_0^2 - \zeta_2 w \sin(w\tau) = 0 \\ &\zeta_1 w - \zeta_2 w \cos(w\tau) = 0 \end{aligned} \tag{17}$$

Simultaneously, using (17), remove the time-delay coefficient τ, and obtain

$$w^4 - 2w^2\omega_0^2 + \omega_0^4 + \zeta_1^2 w^2 - \zeta_2^2 w^2 = 0 \tag{18}$$

To solve further,

$$w_{1,2} = -a^2 \pm \sqrt{a^2 - w_0^4} \tag{19}$$

Thereinto, $a = \frac{\zeta_1{}^2 - \zeta_2{}^2 - 2w_0^2}{2}$. From Equation (17), we obtain

$$\begin{aligned} \tau_1 &= \tfrac{1}{w}(2\mathrm{n}\pi + \arccos\tfrac{\zeta_1}{\zeta_2}) \\ \tau_2 &= \tfrac{1}{w}(2(\mathrm{n}+1)\pi - \arccos\tfrac{\zeta_1}{\zeta_2}) \end{aligned} \tag{20}$$

In Equation (20), n = 0, 1, 2, 3, ... When there is positive damping of the STC, the negative damping caused by the pedestrians' speed and the fundamental frequency of the STC are determined; then, the time-delay coefficient τ corresponds to two values τ_1 and τ_2 in constant crossing. If $\tau_1 < \tau_2$, the STC is stable; if the time-delay coefficient $\tau = \tau_1$, the STC will undergo a Hopf bifurcation, at which point the STC has no real solution, and if the time-delay coefficient $\tau = \tau_2$, the STC will again undergo a Hopf bifurcation, at which point the STC has a real solution. Therefore, changes in the time-delay coefficient τ may affect the lateral vibration of the STC.

4. Numerical Analysis of the Millennium STC Parametric Vibration Considering Time-Delay Effect

4.1. Calculation Parameters Related to the Midspan of the Millennium Bridge

The middle span length is L = 144 m, the width of the STC deck is b = 4 m, the height of the main beam is h = 0.06 m, the elastic modulus is E = 2.1 $\times$ 10^{11} N•m^2, the mass of the STC per meter is m_s = 2000 kg/m, the weight of a pedestrian is m_{sp} = 70 kg, the equivalent cross-sectional region is A = 0.255 m^2, the equivalent tensile stiffness and compressive stiffness are EA = 5.355 $\times$ 10^{10} N•m^2, the dynamic load coefficient for longitudinal walking forces is $a_{h1} = 0.037$, the equivalent bending stiffness is EI = 7.650 $\times$ 10^{10} N•m^2, the dynamic load coefficient for lateral walking forces is $a_{l1} = 0.04$, the dynamic load coefficient related to the vibration speed of the STC is $a_{lv} = 0.7$, the synchronization coefficient for pedestrians is $\lambda = 0.3$, the damping ratio of the STC is $\zeta_0 = 0.007$, and the lateral first-order frequency is 2.4 rad/s.

4.2. Time-Delay Effects on the Dynamic Instability Region in the Midspan of the Millennium STC

Figure 2 shows the relationship between the midspan frequency ratio θ/2Ω and the critical number of pedestrians *N* at the time time-delay coefficient τ = 0 s. It can be seen from the figure that the number of critical rows calculated without considering the time-delay effect *N* = 170 is not much different from the critical number of rows *N* = 178 obtained by Piccardo [8] based on the parametric resonance analysis method, the number of critical pedestrians obtained by the multi-scale method [21], and the number of critical pedestrians *N* = 173 obtained by the midspan field organization [8]. The calculation results show that the equation establishment and solution method in this paper have good accuracy and rationality.

In order to explore the stability characteristics of the left and right border separately, we study them. Figure 3a shows the relationship curve of the midspan left border corresponding to different time-delay coefficients. When the frequency ratio θ/2Ω = 1 is taken in the left border, and the time-delay coefficients τ are taken as 0 s, 0.2 s, 0.4 s and 0.6 s, the corresponding critical number of pedestrians N is 170, 169, 172 and 170, respectively. It was shown that when the STC was in the parametric resonance region, the time-delay effect had little effect on the critical number of pedestrians in the left border. When the frequency ratio θ/2Ω = 0.955 is taken in the left border, and the time-delay coefficients τ are 0 s, 0.2 s, 0.4 s and 0.6 s, the corresponding critical number of pedestrians N is 1773, 1878, 1770 and

1884, respectively. It shows that when the STC is far away from the parametric resonance region, with the increase in the time-delay coefficient, the number of critical pedestrians increases first; then, it decreases and then increases. Obviously, when the STC is far away from the parametric resonance region, the time-delay effect has an effect on the value of the parametric resonance point.

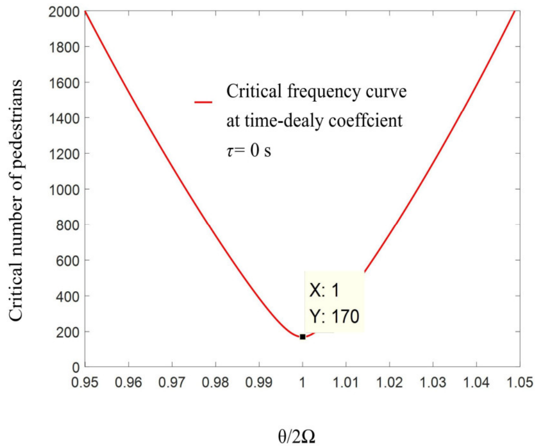

Figure 2. Relation curve between the midspan frequency ratio and critical pedestrian number (time-delay coefficient τ = 0 s).

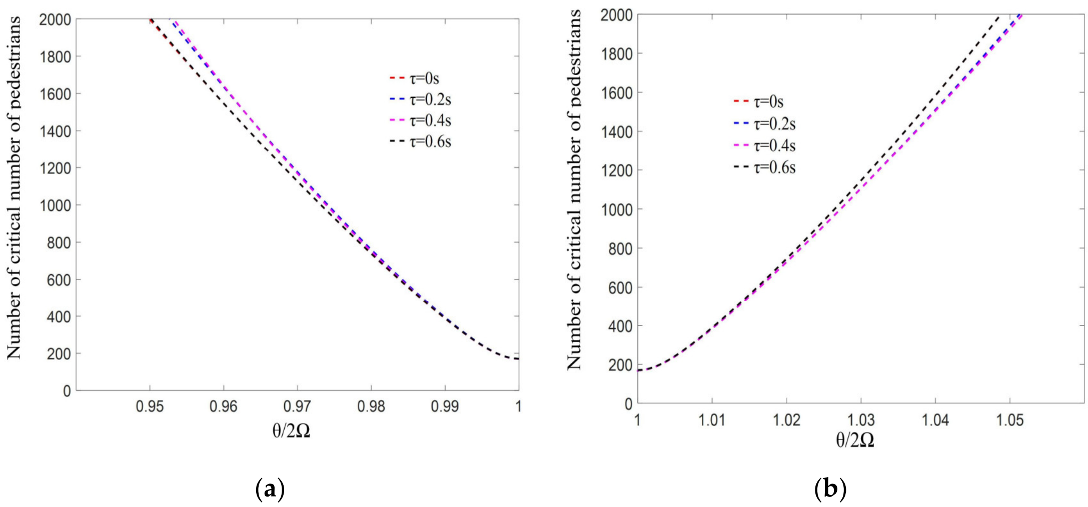

Figure 3. Relationship curve of right border–left border at midspan corresponding to different time-delay coefficients. (**a**) Left border. (**b**) Right border.

Figure 3b shows the relationship curve of the right border of the midspan corresponding to different time-delay coefficients. When the frequency ratio $\theta/2\Omega$ = 1 is taken in the right border, and time-delay coefficients τ are 0 s, 0.2 s, 0.4 s and 0.6 s, the corresponding critical number of pedestrians N is 170, 171, 168 and 170, respectively, indicating that when the STC is in the parametric vibration region, the value of different time-delay coefficients τ has little effect on critical number of pedestrians in the right border. When the frequency ratio $\theta/2\Omega$ = 1.045 is taken in the right border, and the time-delay coefficients τ are taken as 0 s, 0.2 s, 0.4 s and 0.6 s, the corresponding critical number of pedestrians N is 1770, 1792, 1733 and 1798, respectively. The regions of stability and instability on the right border are constantly changing. It is shown that when the STC is far away from the parametric resonance region, the values of different time delay coefficients have a slight influence on the critical number of people.

In order to prove the correctness of the conclusion, by setting the number of pedestrians N on the STC to 50, 170 and 300 people, the nonlinear dynamic response numerical analysis of the midspan parametric vibration of the Millennium STC was carried out under three different working conditions: stable region, critical region and instability region, and the influence of time-delay effect on the dynamic stability of the STC was analyzed. The number of pedestrians and working conditions correspond to the three states of unexcited parameter vibration, excitation parameter vibration critical conditions, and excited parameter vibration.

4.3. Effect of Time-Delay Effect on the Nonlinear Dynamic Response of the Midspan of the Millennium STC

4.3.1. Stable Region

Figure 4a–d show the displacement time course and phase plane curves for the midspan of the Millennium STC for the number of pedestrians N = 50 and the time-delay coefficients of 0 s, 0.2 s, 0.4 s, and 0.6 s. The corresponding displacement time course and phase plane curves differ for different initial conditions. When the time-delay coefficient $\tau = 0$ s, the lateral displacement time course curve shows the characteristics of first attenuation and then equal amplitude vibration. Each closed phase trajectory of the corresponding phase plane curve undergoes attenuation oscillation and finally tends to the equilibrium state, and the trajectory around the limit ring converges to the coordinate origin, which is a convergent and attenuated non-reciprocating motion.

The figure shows that the STC has not yet excited the parametric vibration at this time and is in a stable transient vibration state at this time, and the coordinate origin is the stable focus. Comparing Figure 4a–d, when the time-delay coefficient τ changes from 0 s, 0.2 s, 0.4 s and 0.6 s, the corresponding lateral displacement amplitude changes, and the shape of the phase plan diagram has obvious changes.

4.3.2. Critical Region

Figure 4e–h show the displacement time course and phase plane curves of the midspan of the Millennium STC for the number of pedestrians N = 170 and the values of time-delay coefficient 0 s, 0.2 s, 0.4 s, and 0.6 s. When the time-delay coefficient $\tau = 0$ s, the lateral displacement time course curve shows a transition from “linear variation” to “exponential dispersion”. Each phase trajectory corresponding to the phase plane curve has the characteristic of being half far away and half convergent to the coordinate origin. It indicates that the STC begins to excite parametric vibration, which is in a semi-stable state; that is, the STC is in a stable to unstable transition stage.

Comparing Figure 4a–d, when the time-delay coefficient τ changes from 0 s, 0.2 s, 0.4 s and 0.6 s, the lateral displacement amplitude and the phase trajectory of the phase plane change significantly, indicating that the existence of the time-delay effect will not only affect the time when the STC reaches a stable amplitude but also change the motion state of the STC. Therefore, when the STC is in a critical region, the time-delay effect will affect its lateral vibration. When the time-delay coefficient $\tau = 0.2$ s, the corresponding displacement amplitude is smaller than that of other times, indicating that there is an appropriate time-delay value for the STC, which can play a role in suppressing its lateral vibration, which can be achieved by adjusting the material, thickness and length of the bridge deck material of the STC.

4.3.3. Regions of Instability

When the number of pedestrians on the bridge $N = 300$ and the time-delay coefficient values are 0 s, 0.2 s, 0.4 s and 0.6 s, the displacement time course curve and phase plane curve of the midspan of the Millennium STC are shown in Figure 4i–l. The time-delay coefficient $\tau = 0$ s at that time, and the lateral displacement time course curve shows the characteristics of “equal amplitude vibration” first, then “exponential divergence” and then “chaotic amplitude vibration”. The phase plane curve shows that the phase trajectories near the limit ring all diverge from the coordinate origin, and each phase trajectory is far away from the coordinate origin, which is accompanied by a state of chaotic motion. It can be found that the time-delay coefficient τ will not change the displacement time course curve and phase plane curve of the STC when the four values are 0, 0.2, 0.4 and 0.6. This is because STC in the parametric resonance region, even if there is a slight time-delay effect, will gradually be overwhelmed by the violent parametric resonance over time.

4.4. Analysis of the Impact of Time-Delay Effect on the Midspan of the Millennium STC

The variation pattern of the number of pedestrians on the midspan of the Millennium STC under the influence of the time-delay effect is analyzed according to the central flow-form theorem and normality theory. Figure 5 shows that when n = 0, there are two solutions in the time-delay coefficient τ corresponding to the critical number of people, and the characteristic root is crossing.

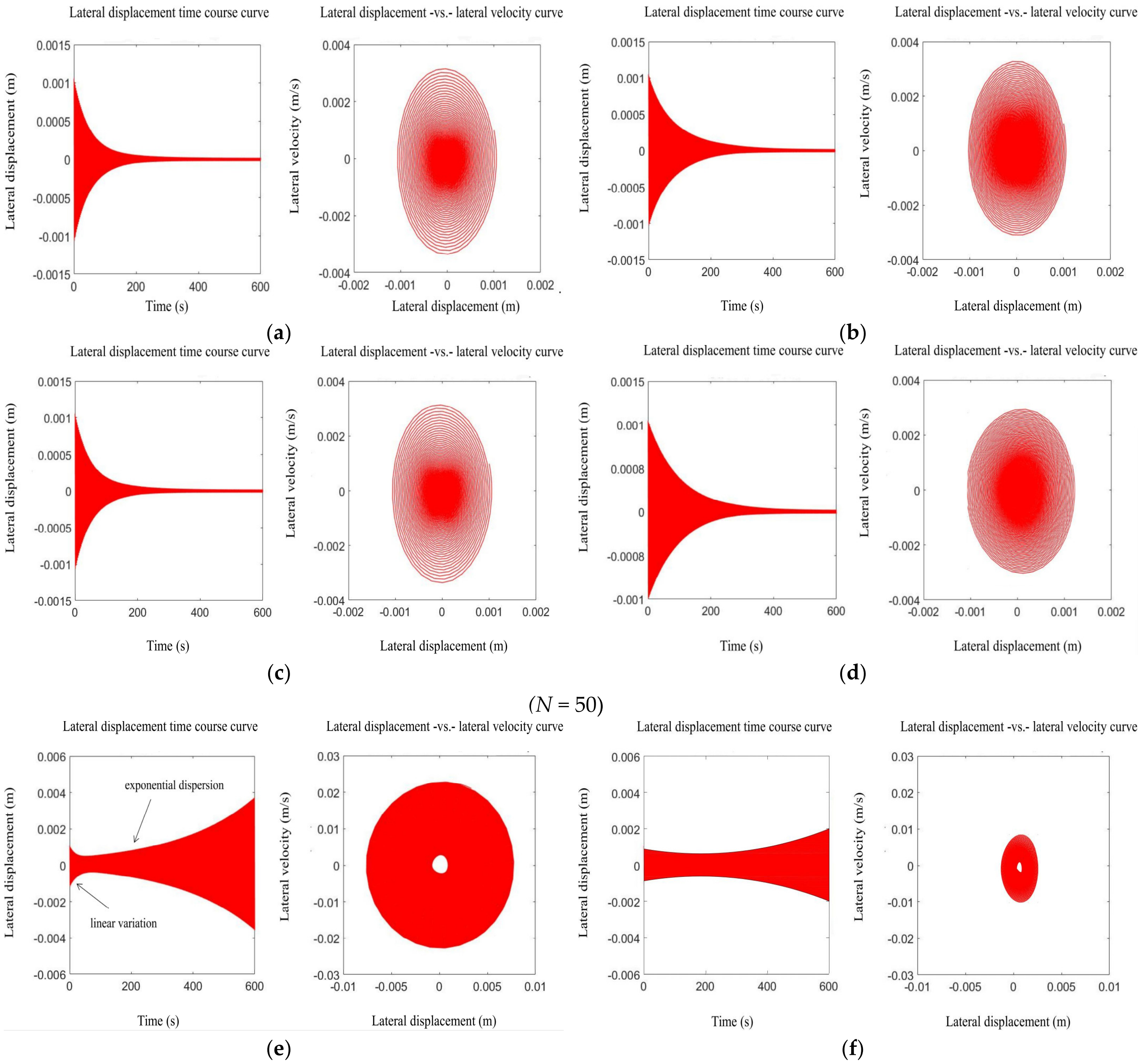

Figure 4. *Cont.*

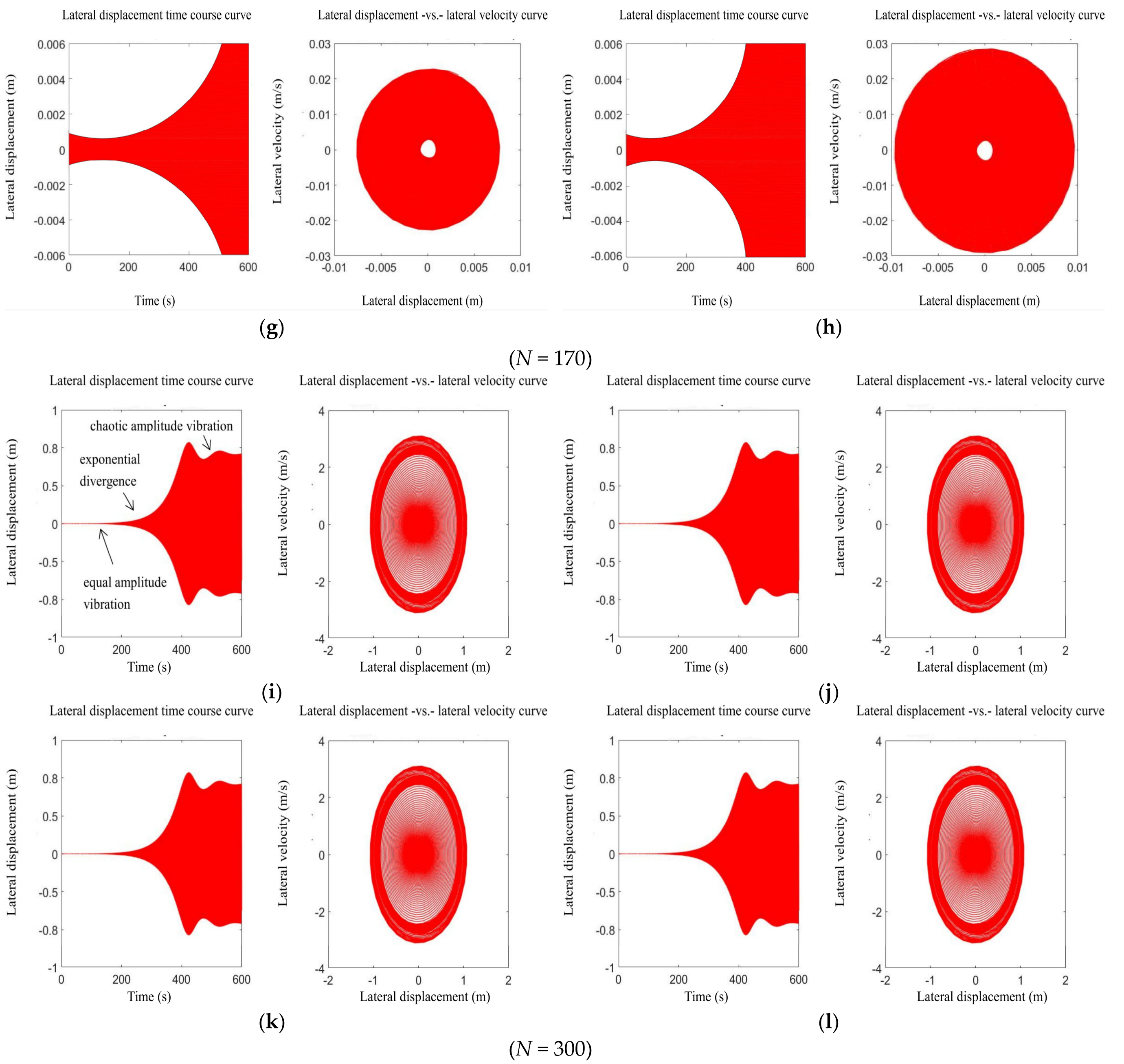

Figure 4. Displacement time-course curve and phase plane curve (N = 50, 170, 300). (**a**) τ = 0 s. (**b**) τ = 0.2 s. (**c**) τ = 0.4 s. (**d**) τ = 0.6 s. (**e**) τ = 0 s. (**f**) τ = 0.2 s. (**g**) τ = 0.4 s. (**h**) τ = 0.6 s. (**i**) τ = 0 s. (**j**) τ = 0.2 s. (**k**) τ = 0.4 s. (**l**) τ = 0.6 s.

From Figure 5, as the time-delay coefficient τ increases, the equilibrium point on the midspan of the Millennium STC is destabilized due to the co-existence of Hopf bifurcation. That is, when the STC is in the nonparametric resonance region and the critical region, the number of pedestrians N on the STC will correspond to a pair of mutually staggered critical bifurcation time-delay values, and the critical bifurcation behavior of this time-delay effect will cause the STC to cross from a stable state to an unstable state and back to a stable state.

As number of pedestrians N increases, τ_1 first increases and then decreases; τ_2 first decreases and then increases. When the number of pedestrians exceeds 170, the time-delay coefficient τ has no real solution, i.e., the violent parametric resonance phenomenon of the STC overwhelms the delayed effect of the time-delay effect, which is consistent with the solution of the critical number of pedestrians N = 170 for the midspan parametric resonance in the Millennium STC obtained from the above theoretical calculation. When $\tau > \tau_1$, the positive damping effect on the midspan of the Millennium STC suppresses the lateral vibration of the STC; when $\tau > \tau_2$, the negative damping effect caused by the pedestrians velocity intensifies the lateral vibration on the midspan of the Millennium STC and exhibits the characteristic that the lateral vibration of the STC increases with the increase in the time-delay coefficient τ.

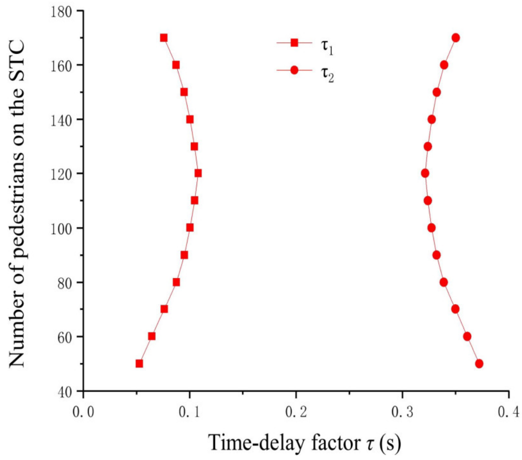

Figure 5. Bifurcation diagram of time-delay effect and pedestrians number on the STC.

5. Conclusions

In this paper, the lateral vibration of the STC is studied by combining the engineering example of the midspan of the Millennium STC and the experimental research of Dallard, and the Bolotin method is used to solve the second-order approximate solution of the critical frequency curve of the Millennium STC, and the calculation results are more consistent with the existing research results, which proves the correctness of the selection method. Then, a program is written to explore the influence of the time-delay effect on the lateral nonlinear dynamic response of the midspan of the Millennium STC. Finally, combined with the principle of nonlinear Hopf bifurcation, the stability of the equilibrium point of the midspan of the Millennium STC is studied. The following conclusions were obtained:

(1) When there is a time-delay effect, the frequency ratio $\theta/2\Omega = 1$, the regional boundary size, shape and rotation center of its dynamic stability do not change, and the value of the time-delay coefficient has no effect on the critical number of pedestrians on the STC in the parametric resonance region. As the frequency ratio $\theta/2\Omega$ gradually moves away from 1, the time-delay effect slightly affects the value of the critical number of pedestrians, and the effect becomes more significant as the frequency ratio $\theta/2\Omega$ is farther away from 1.

(2) For STC in nonparametric resonance regions, the time-delay coefficient will affect the lateral dynamic stability of the STC. When the STC begins to excite the parametric resonance phenomenon, the existence of the time-delay effect will change the time for the STC to reach a stable amplitude, and the existence of a suitable time-delay value on the STC can suppress the lateral vibration of the STC. When the STC generates severe parametric vibration, the value of the time-delay coefficient will not affect the nonlinear dynamic response of the STC.

(3) As a dynamic control parameter, the time-delay coefficient will affect the complex dynamic behavior of the parametric vibration of the STC. For STC in the non-parametric resonance region and critical region, there is a pair of staggered critical bifurcation time-delay coefficients, and the number of pedestrians N on different STC corresponds to different critical time-delay values τ_1 and τ_2, and different time-delay coefficients will change the vibration response of the midspan of the Millennium STC; the instant time-delay effect causes the pedestrian bridge to cross between a steady state and an unstable state.

Author Contributions: Conceptualization, Z.C., J.W., D.D., W.D., S.C. and H.L.; methodology, Z.C., J.W., D.D., W.D., S.C. and H.L.; software, Z.C., D.D., S.C. and H.L.; validation, Z.C., J.W., S.C. and H.L.; formal analysis, Z.C., J.W., D.D., W.D. and S.C.; investigation, Z.C., D.D., W.D., S.C. and H.L.; resources, Z.C., D.D., W.D. and H.L.; data curation, Z.C., J.W. and D.D.; writing—original draft preparation, Z.C., J.W., D.D., W.D., S.C. and H.L.; writing—review and editing, Z.C., J.W. and L.L.; visualization, Z.C., J.W. and D.D.; supervision, Z.C., J.W. and D.D.; project administration, Z.C., J.W. and D.D.; funding acquisition, Z.C., H.L. and L.L. All authors have read and agreed to the published version of the manuscript.

Funding: The National Natural Science Foundation of China (51908146). Energy Collection, Transformation and utilization in civil engineering (G2022030014L). The Overseas Famous Teachers in Guangdong Province (Energy Harvesting and its Applications in Civil Engineering). Young innovative talents project of regular universities in Guangdong Province (2018KQNCX278), the Innovation Project of Guangdong Graduate Education (2019JGXM101).

Data Availability Statement: The data presented in this study are available on request from the corresponding author.

Acknowledgments: The authors would like to thank all partners of School of Transportation and Civil Engineering & Architecture, Foshan University for their contribution to this research, with specific thanks to all partners in China Construction Steel Structure Guangdongcorp. who have collected the data and to the partners at the Guangdong Nanhai Construction Investment Development Co. For their help with the processing of the data. Additionally, the authors thank all partners at School of Civil Engineering, Southeast University, Nanjing who have been extremely cooperative in their involvement in this research.

Conflicts of Interest: The authors declare no conflict of interest.

References

1. Dey, P.; Narasimhan, S.; Walbridge, S. Reliability-based assessment and calibration of standards for the lateral vibration of pedestrians bridges. *Eng. Struct.* **2021**, *239*, 112–271. [CrossRef]
2. Peng, J.L.; Luo, X.Q.; Zhang, Q.L. Analysis and control of human-induced vibration response of a STC supported by an arch cable. *Build. Struct.* **2017**, *47*, 569–573.
3. Casciati, F.; Casciati, S.; Faravelli, L. A contribution to the modelling of human induced excitation on pedestrians bridges. *Struct. Saf.* **2017**, *66*, 51–61. [CrossRef]
4. Song, Z.G.; Huan, Y. Estimating the critical number of lateral vibrations of STC structures using the social force model. *J. Vib. Eng.* **2014**, *27*, 233–237.
5. Wang, D.Y.; Wu, C.Q.; Zhang, Y.S.; Li, S.W. Study on vertical vibration control of long-span steel footbridge with tuned mass dampers under pedestrians excitation. *J. Constr. Steel Res.* **2019**, *154*, 84–98. [CrossRef]
6. Qin, J.W. Human-structure interaction is based on a bipedal walking model. *Beijing Jiaotong Univ.* **2013**, *07*, 150.
7. Luongo, A.; Piccardo, G. Linear instability mechanisms for coupled translational galloping. *J. Sound Vib.* **2005**, *288*, 1027–1047. [CrossRef]
8. Firus, A.; Kemmler, R.; Berthold, H.; Lorenzen, S.; Schneider, J. A time domain method for reconstruction of pedestrians induced loads on vibrating structures. *Mech. Syst. Signal Process.* **2022**, *171*, 108–887. [CrossRef]
9. Bassoli, E.; Gambarelli, P.; Vincenzi, L. Human-induced vibrations of a curved cable-stayed footbridge. *J. Constr. Steel Res.* **2018**, *146*, 84–96. [CrossRef]
10. Venuti, F.; Bruno, L. Mitigating human-induced lateral vibrations on footbridges through walkway shaping. *Eng. Struct.* **2013**, *56*, 95–104. [CrossRef]
11. Jia, B.Y.; Yan, Q.S.; Yu, X.L. Stability analysis of pedestrian-induced large lateral vibration on a footbridge. *Eng. Mech.* **2019**, *36*, 155–164. [CrossRef]
12. Piccardo, G.; Tubino, F. Parametric resonance of flexible footbridges under crowd-induced lateral excitation. *J. Sound Vib.* **2008**, *311*, 353–371. [CrossRef]
13. Xia, Y.; Fujino, Y. Auto-parametric vibration of a cable-stayed-beam structure under random excitation. *J. Eng. Mech.* **2006**, *132*, 279–286. [CrossRef]
14. Wei, X.X.; Peter, V.D.B.; Guido, D.R.; Katrien, V.N. A simplified method to account for the effect of human-human interaction on the pedestrians-induced vibrations of footbridges. *Procedia Eng.* **2017**, *199*, 2907–2912. [CrossRef]
15. Gabriella, M.M.; Lai, E.; Giulia, L. Coupled Analysis of STC-pedestrians dynamic interaction. *Eng. Struct.* **2018**, *176*, 127–142.
16. Lu, D. *Response Analysis and Vibration Assessment of Tibetan Ancient Structures under Crowd Loading*; Beijing Jiaotong University: Beijing, China, 2017.
17. Hu, H.Y. *Applied Nonlinear Dynamics*; Aviation Industry Press: Shanghai, China, 2000.

18. Dillard, P.; Fitzpatrick, T.; Flint, A. London Millennium Brigde: Pedestrians-induced Lateral Vibration. *J. Bridge Eng.* **2001**, *06*, 412–417. [CrossRef]
19. Bolotin, V.V. *The Dynamic Stability of Elastic Systems*; Aerospace Corp el: Segundo, CA, USA, 1962.
20. Meyer, R.B.K.R. Theory and Applications of Hopf Bifurcation. *Siam Rev.* **2006**, *24*, 498–499. [CrossRef]
21. Zhou, C.; Yan, Q.S.; Deng, D.Y.; Chen, Y.J.; Jia, B.Y.; Yu, X.L. Study on nonlinear lateral parametric vibration of footbridges under crowd excitation. *Vib. Shock* **2018**, *37*, 47–51.